Available online at www.sciencedirect.com
ScienceDirect
Journal of the European Ceramic Society 26 (2006) 3717–3723
www.elsevier.com/locate/jeurceramsoc

Synthesis and characterization of nanocrystalline $SrBi_2Nb_2O_9$ ferroelectric ceramics using TEA as the polymeric matrix

D. Dhak, S.K. Biswas, P. Pramanik *

Department of Chemistry, Indian Institute of Technology Kharagpur, Kharagpur 721302 India

Received 2 September 2005; received in revised form 21 November 2005; accepted 3 December 2005
Available online 18 January 2006

Abstract

The processing conditions, reaction mechanism, fine structure of the powders, microstructure, and dielectric properties of $SrBiNb_2O_9$ (SBN) were systematically studied. A relative density of >80% was obtained using a two-step sintering process at moderate pressure. XRD showed that a single phase with the layered perovskite structure of $SrBi_2Nb_2O_9$ (SBN) was formed after calcining at 600 °C. No intermediate phase was found during heat treatment at and above 600 °C. The crystallite size (D) and the effective strain (η) were found to be 38.8 nm and 0.01475, respectively, while the particle size obtained from TEM was laid between 25 and 36 nm. SEM revealed that the average grain size after sintering at 900 °C for 4 h was 0.67 μm. Dielectric constant and corresponding tangent loss were measured in the frequency range from 1 kHz to 1 MHz from which the Curie temperature (T_c) was found to be at 450 °C.

Keywords: Precursors-organic; Perovskites; Electron microscopy; Dielectric properties; $SrBi_2Nb_2O_9$

1. Introduction

Previous research has focused on $Pb(Ti, Zr)O_3$ (PZT), but one of the current problems with PZT is the fatigue resistance of the material. PZT thin films tend to degrade after 10^6 to 10^8 cycles of full polarization switching.[1] Bismuth layered perovskite materials have high fatigue resistance and are able to withstand 10^{12} erase/rewrite operations[2] and therefore have attracted an increasing attention for NvRAM application.[3] The crystal structure and chemical composition of these layered perovskites were systematically studied by Aurivillius[4] in the 1950's with a general formula of $(Bi_2O_2)^{2+}(A_{m-1}B_mO_{3m+1})^{2-}$, consisting of m-perovskite units sandwiched between bismuth oxide layers called the family of bismuth layered structured ferroelectrics (BLSFs),[5] where A and B are the two types of cations that enter the perovskite unit. A is Bi^{3+}, Ba^{2+}, Sr^{2+}, Pb^{2+}or K^{1+}; B is Ti^{4+}, Ta^{5+}, Nb^{5+}, Mo^{6+} or W^{6+} and $m = 1$–6.[3] The crystal structure is built up of two perovskites-like layers, infinite in two dimensions, alternating with a layer of $(Bi_2O_2)^{2+}$ along the c-axis. The O–Nb–O chains of the perovskites along the same axis are interrupted to this class have been found to have wide spread applications in a variety of ferroelectric-based devices.[2,3] However, the conventional way to synthesize SBT and SBN based on the solid-state reaction at high temperatures (typically >1200 °C)[2] is not suitable for ferroelectric applications, since they suffer from relatively high processing temperature, relatively low spontaneous polarization, and relatively high dielectric loss.[6,7] Much research has been reported in the open literature aimed at improving the dielectric and ferroelectric properties of such materials.[8,9]

The phase formation temperature, chemical homogeneity, phase purity and electrical properties of multicomponent electroceramic materials like SBN and SBT are highly dependent on the cation homogeneity in the oxide precursor.[10] In this respect the sol–gel synthesis,[9,11–14] and the Pechini-type polymerizable complex (PC)[15] are extremely useful. Unfortunately, the non-aqueous based solution methods (i.e. the alkoxide based solution methods using organic solvents)[16] experience hindrance in the synthesis of ceramics that contain niobium (V) ions because of the cost, and moisture sensitivity of the starting materials (such as niobium ethoxide and other alkoxides). On the other hand, the alternative aqueous based chemical processes get complicated due to scarcity of water-soluble salts of niobium and easy hydrolysis of the available ones (such as $NbCl_5$).

* Corresponding author. Tel.: +91 3222 283322; fax: +91 3222 255303.
E-mail addresses: pramanik@chem.iitkgp.ernet.in, panchanan_123@yahoo.com (P. Pramanik).

0955-2219/$ – see front matter © 2005 Elsevier Ltd. All rights reserved.
doi:10.1016/j.jeurceramsoc.2005.12.002

In the present work, we report the use of water soluble, coordinated complex of niobium-tartarate as a starting material for the preparation of nanocrystalline $SrBi_2Nb_2O_9$ powders through an aqueous based chemical process. Niobium-tartarate is stable in aqueous medium and is appropriate for the preparation of multi-component oxide systems comprising Nb(V) ions. The route involves the complete dehydration of an aqueous precursor solution that have the constituent metal ions in solution through formation of coordinated complexes with readily available, inexpensive compounds, such as, tartaric acid, ethylenediamine tetraacetic acid (EDTA) and triethanolamine (TEA).

2. Experimental

Chemical required for this synthesis are $Sr(NO_3)_2$ (MERCK, India; 99.99%), $Al(NO_3)_3 9H_2O$ (MERCK, India; GR grade), $Bi(NO_3)_3 5H_2O$ (Aldrich; 99.999%), Nb_2O_5 (Aldrich; 99.99%), TEA (triethanolamine) (MERCK, India; GR grade), EDTA (ethylenediamine tetraacetic acid), HNO_3 (65%) (MERCK, India; GR grade), and NH_4OH (25%) (MERCK, India; GR grade).

2.1. Preparation of water-soluble Bi- and Sr-EDTA complex

Bismuth nitrate, $Bi(NO_3)_3 5H_2O$ (0.1 mol), and ethylenediamine tetraacetic acid, abbreviated as H_4-EDTA (0.1 mol), were mixed with 300 ml of water with stirring to form a colloid of Bi-species hydrolyzed. The colloidal solution was treated with 70–80 ml of 28 wt.% ammonia solutions to form a water-soluble Bi-EDTA complex. The pH of the solution was adjusted to seven drop wise using 6 mol l^{-1} HNO_3, followed by addition of water to prepare 0.2 mol l^{-1} Bi-EDTA stock solutions. The corresponding stock solution of Sr-EDTA was prepared starting from strontium nitrate, $Sr(NO_3)_2$, in the way similar to that of the Bi-EDTA. The metal content was determined by ICP (inductive coupled plasma) analysis.

2.2. Preparation of water-soluble Nb-tartarate complex

Aqueous solutions of the niobium tartarate complex were prepared in the laboratory starting from its hydrous oxide. To begin with, the niobium oxide (Nb_2O_5) was dissolved in HF (>7 M) by warming the mixture over a water bath for 24 h to obtain a clear solution of the niobium-fluoride complex (i.e. NbF_5^{2-} complexes). The hydrous niobium oxide ($Nb_2O_5 \cdot nH_2O$) was then precipitated out from the clear solution of the niobium-fluoride complex by the addition of aqueous solutions of dilute (25%) ammonia. The precipitate of $Nb_2O_5 \cdot nH_2O$ was filtered, washed with 5% ammonia solution to make it fluoride free and then assayed at 1000 °C for 2 h to estimate niobium oxide The required amount of hydrous niobium oxide was then taken and slowly dissolved in aqueous solution of tartaric acid (2 M per unit mol of niobium ion) with continuous stirring on a magnetic stirrer to obtain the stock of the clear, aqueous solution niobium tartarate. The entire process for obtaining the aqueous of niobium tartarate has been depicted through a flow chart in Fig. 1.

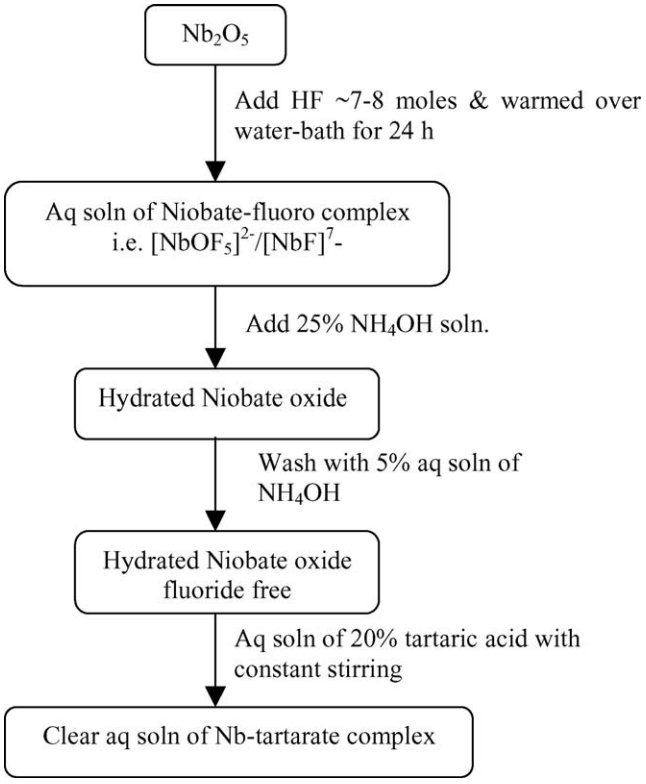

Fig. 1. Schematic representation of the preparation of niobate-tartarate complex.

2.3. Preparation of $SrBiNb_2O_9$ via an aqueous solution route

For the preparation of $SrBiNb_2O_9$ appropriate volumes of the Sr-EDTA, Bi-EDTA, and Nb-tartarate complexes were taken from their respective stock solutions, in accordance with the desired stoichiometries, and mixed together. As shown in Fig. 2, the precursor solution was subsequently obtained by adding TEA, which acts as a complexing agent,[17] to the resultant mixture of the metal ion complexes. 4.5 wt.% of extra Bi-EDTA was taken to avoid any possible weight loss during heat treatment. To avoid any chances of precipitation of the metal ions from the precursor solution, the amount of TEA added was always kept in excess (i.e. 3 mol ratios with respect to per mol of the total metal ions) for the required stoichiometry and the pH of the solution mixture was maintained at 6. The entire precursor solution was then rapidly evaporated by heating at ~200 °C, complete dehydration of the precursor solution was accompanied by the decomposition of the metal complexes followed by the generation of a voluminous, carbonaceous mesoporous precursor mass, which was ground to fine powder and subsequently calcined at different temperatures (500–800 °C) for 2 h to result in the desired nano-sized SBN powders. The details of the mechanism of solution decomposition method using TEA has been discussed in a recent communication by our group.[18]

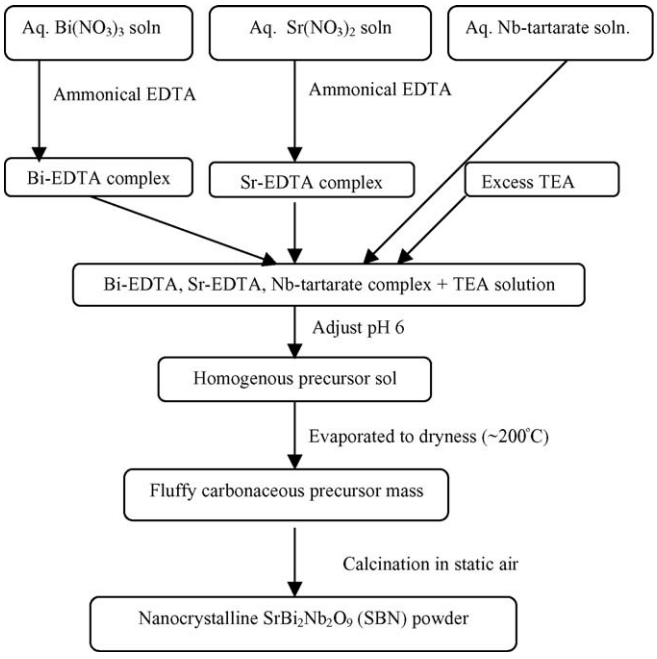

Fig. 2. Schematic representation of the precursor solution method for the synthesis of $SrBi_2Nb_2O_9$ powders.

3. Characterizations

3.1. Sample characterization

Thermo gravimetric (TG) and differential thermal analyses (DTA) (Model DT-40, Shimadzu Co., Japan) of the precursor powders were carried out in static air at a heating rate of 10 °C/min upto 1000 °C using alumina crucible. The precursor powders were heated in static air in a programmable furnace (Lenton furnace, Welland Industrial Estate, England) at a heating rate of 10 °/min in order to obtain polycrystalline SBN powder. XRD (Model: Philips PW1710) was used to determine the formation of the desired layered perovskite phase, for the powders. The XRD spectrum of Si crystal was used as a standard to calibrate the scanning angles. Cu Kα was used as target material. The step size of the scan was 0.04° 2θ, with a scanning speed of 0.02° 2θ/s. The lattice planes (0 2 0) and (1 1 5) were chosen for the lattice constant calculation. The fine structure of the prepared powders was analyzed by the TEM (Model: TM–300, Philips). The sample was prepared by sonnicating a pinch of the sample for half an hour using acetone as dispersing solvent and then was taken on a carbon coated (50 nm thickness) copper grid of 300 mesh. The as-prepared powder was mixed with one drop of 1 wt.% solution of polyvinyl alcohol and uniaxially pressed at room temperature for one minutes at the pressure 190 MPa/cm^2. The sintering of the pressed pellets was done with help of the same furnace, which were used for the phase formation of the precursor powders. The density of the sintered pellets was measured by pycnometer by Archimedes principle using xylene as the solvent. The microstructure of the sintered sample was analyzed by SEM (Mode: JEOL JSM–5800) taken on the polished surface. The polished surfaces were coated with gold by sputtering before taking the micrograph.

3.2. Dielectric constant measurements

The dielectric constant and the tangent loss measurements were done on the polished pellet samples as a function of frequency (1 kHz to 1 MHz) at various temperatures (300–500 °C), using an LCR meter (HIOKI, model 3532, Japan). For this purpose the sintered ceramic pellets were polished to have flat and parallel surfaces. The thickness and area of the samples were about 25 mm and 100 mm^2, respectively. The polished surfaces of the sample pellets were electroded by silver paste on both sides, and cured at 300 °C for 2 h. A constant heating rate of 1 °C/min was maintained for making the above physical property measurements. The capacitance, Cp and the loss tangent, tan δ were recorded simultaneously at the frequencies 1 kHz, 100 kHz, and 1 MHz. The dielectric constant (ε) was calculated according to the following equation:

$$\varepsilon = \frac{\mathrm{Cp}d}{\varepsilon_0 A} \quad (1)$$

where A and d are the electrode area and thickness of the ceramic pellet, respectively, and ε_0 is the free space permittivity ($\sim 8.85 \times 10^{-12}$ F/m). The dielectric constants that are reported in this paper are uncorrected for porosity and the influence of which the dielectric properties are under systematic investigation, the details will form a separate communication.

4. Results and discussions

4.1. Thermal study

The DTA curves in Fig. 3 revealed an exothermic thermal affect for SBN precursor powders with their respective peak around 380–500 °C. The exothermic peak could be assigned to the oxidation of carbonaceous remains from the decomposed metal-complexes and TEA. The entire thermal effect was accompanied by the evolution of various gases (such as CO, CO_2, NH_3, water vapor, etc.), which was manifested by a single step weight loss in the TG curves shown in Fig. 3. No clear exothermic peak corresponding to $SrBiNb_2O_9$ crystallization was found. Above 500 °C, there was no significant thermal effect observed in DTA curves and the corresponding TG curves showed no

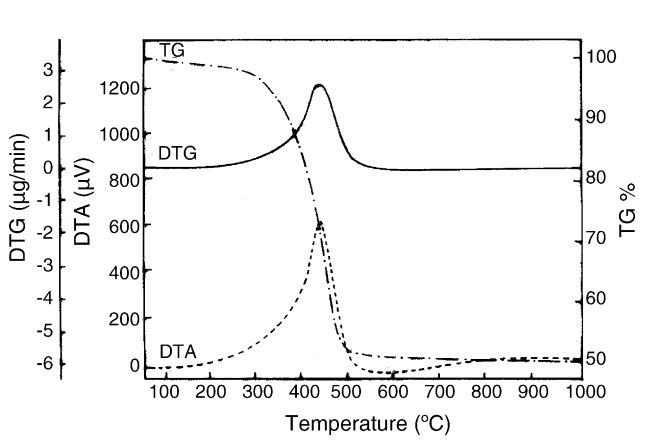

Fig. 3. Simultaneously recorded DTA/TG for $SrBi_2Nb_2O_9$ precursor.

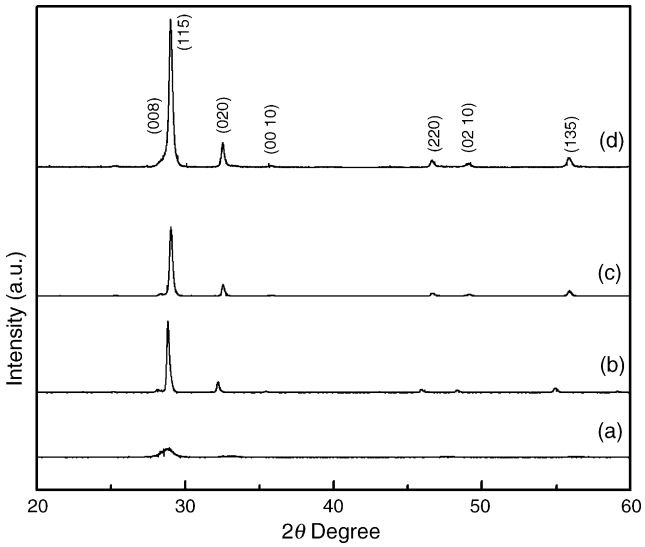

Fig. 4. XRD spectra of the $SrBi_2Nb_2O_9$ ferroelectric ceramics calcined at: (a) 500; (b) 600; (c) 700; and (c) 800 °C for 2 h in static air.

weight loss, implying the complete volatilization of carbon compounds.

4.2. Formation of single-phase layered perovskite

The phase formation temperatures were detected from the XRD spectra obtained at different calcination temperatures ranging from 500 to 800 °C for 2 h as shown in Fig. 4 in the 2θ range of 20–60°. The peaks were indexed with reference to the JCPDFS file no. 49-0607; $\lambda = 1.54056$. The XRD studies revealed that the virgin precursors were amorphous. The broad halos in the diffractogram characterized the X-ray amorphous nature, which persisted up to the calcination temperatures of 500 °C (Fig. 4(a)). Products after calcining the powder above 500 °C were crystalline. The XRD patterns of the sample calcined at 600, 700 and 800 °C (Fig. 4(b), (c) and (d), respectively) showed no reflections, which match (JCPDFS file no. 49-0607) those of a fluorite structure of $SrBiNb_2O_9$.[11,19] So, the sample completely converted to the ferroelectric Perovskite $SrBi_2Nb_2O_9$ just after heating at 600 °C for 2 h. From this observation, it proves that no fluorite intermediate phase[19] prior to the crystallization of the Perovskite has occurred. No pyrochlore phase has formed at any stage of the heat-treatment in our SBN synthesis. It has been postulated[20] that loss of Bi leads to the formation of a non-ferroelectric pyrochlore phase generally causes depletion Bi compared to the ferroelectric Perovskite phase. To avoid any possibility of formation of Bi-deficient pyrochlore phase to the desired ferroelectric Perovskite phase,[19] some precautions are necessary for the preparation of SBN, which include:

1. The processing temperature should be set as low as possible to minimize loss of Bi during the heat-treatment.
2. The precursor used for SBN should be like the one in which the constituent metal components were dispersed as homogeneously as possible, to block the opportunity of a partial volatilization of Bi prior to the formation of the strictly stoichiometric SBN.
3. To compensate any possible weight loss, chemical were taken with desired ratios with an excess of 4.5 wt.% of Bi-EDTA.

In view of the fact that the perovskites SBN phase has completely formed at 600 °C from the amorphous phase with formation of neither any fluorite phase nor a pyrochlore phase (Fig. 4), it could be concluded that no significant volatilization of Bi has occurred. This might in turn indicate that the extent of homogeneity with respect to distribution of metal ions in our precursor was satisfactory for the low temperature synthesis of SBN.

This relatively lowering in the required external heat-treatment temperatures for the formation of the single phase perovskite SBN phase through the present method indicated the presence of small atomic clusters of appropriate chemical homogeneity in the amorphous precursors that facilitated the crystallization. Average crystallite sizes (Table 1) after the sample calcined at different temperatures for the SBN powders were calculated from XRD peak broadening using the Debye–Scherrer's equation.[21] The values in all the SBN compositions were observed to be increasing with rise in the calcination temperature. The lattice constants and single unit cell volumes were calculated from the XRD spectra with Si reference peaks (not shown here) were found to be $a = 0.548$ nm, $b = 0.548$ nm, $c = 2.535$ nm and unit cell volume $= 0.76127$ nm^3 which are in close agreement with the reported values $a = 0.5523$ nm, $b = 0.5513$ nm, $c = 2.512$ nm and unit cell volume = 0.7648 (JCPDF file no. 49-0607). Information on crystallite size (D) and the effective strain (η) were obtained from the full widths at half maximum (FWHM) of the diffraction peaks obtained after calcining the precursor powder at phase formation temperature at 600 °C. After applying the correction for instrumental broadening with respect to standard silicon, the FWHMs (Eq. (2)) can be expressed by the following equation assuming particle size and strain profiles (Eq. (3)) are of Gaussian type:

$$(\beta^{Ob})^2 = (\beta^p)^2 + (\beta^s)^2 \quad (2)$$

or,

$$(\beta_i \cos\tfrac{\theta}{\lambda})^2 = \left(\frac{1}{D}\right)^2 + (\eta \sin\tfrac{\theta}{\lambda})^2 \quad (3)$$

where β_i is the integral of FWHM (expressed in radians); β^p the FWHM considering the particle size effect; β^s the FWHM due to strain; θ half incident angle of the X-ray; λ the wave length of the target material.

Table 1
Average crystallite sizes in $SrBi_2Nb_2O_9$ powders calcined at their respective crystallization temperatures

Sample	Calcination temperature (°C)	Average crystallite size (nm)
$SrBi_2Nb_2O_9$	600	24
	700	27
	800	31

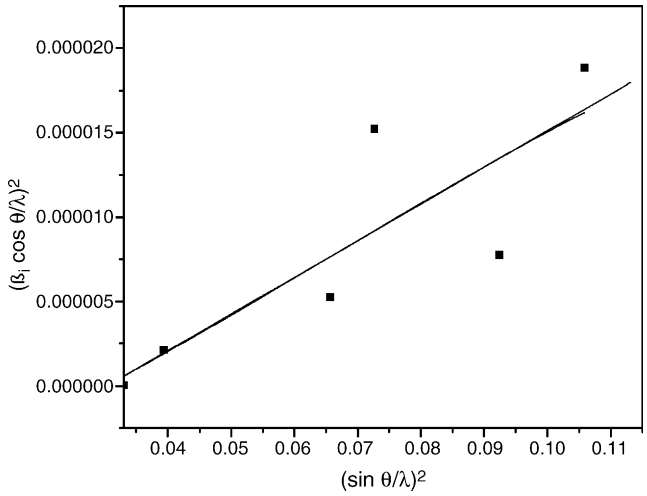

Fig. 5. $(\beta_i \cos\theta/\lambda)^2$ vs. $(\sin\theta/\lambda)^2$ for $SrBi_2Nb_2O_9$ whose $\theta/2\theta$ scans are shown in Fig. 4(b).

Fig. 5 shows the plot of $(\beta_i \cos\theta/\lambda)^2$ versus $(\sin\theta/\lambda)^2$. From the slope of the best fitted line and the intercept at $x = 0$, the effective strain (η) and the crystallite size (D) were found to be 0.001475 and 38.8 nm, respectively. Essentially the sample shows the absence of any significance strain.

4.3. Sintering behavior

The two-step sintering process was applied to all the samples studied. The purpose of the first-step sintering (or calcining) was to form a layered perovskite phase at relatively low temperatures (600 °C). The second sintering step conditions were used to prepare samples for characterizations of microstructure and property after making the pellets from the calcining powders at pressure 190 MPa at room temperature. The pressed pellets were subjected to the conventional solid state sintering process in static air at 900 °C for 5 h. The densities of the sintered pellets were determined by liquid displacement using a pycnometer. Xylene, the density of which is 0.87 g/cm^3 was used as the liquid media. The average density obtained for SBN was 84% of the theoretical value. For all the samples, the overall weight loss was found to be ∼2.5 wt.%, less than the extra amount of bismuth oxide added into the system during the powder preparation, and is presumably caused by the high vapor pressure of bismuth oxide. However, the presence of more bismuth content was seen to promote the densification of the SBN samples appreciably by lowering the sintering temperatures. During the first sintering step, or calcining, bismuth oxide reacted with other constituent oxides and formed a layered perovskite. There would be very little reacted bismuth oxide left for the second sintering step. Therefore, there might be a very small fraction of liquid phase sintering in the second sintering step.

4.4. Fine structure

The bright field TEM (Fig. 6(a)) for $SrBi_2Nb_2O_9$ composition was taken after calcinations of the precursor powders at their phase formation temperature of 600 °C. The bright field TEM micrograph represented the basic powder morphology in the sample, where the smallest visible isolated spot can be identified with particle/crystallite agglomerates.

From the TEM study of the SBN powders, it was observed that the particles have an almost-spherical morphology with narrow particle-size distribution. The average particle diameters lay between 25 and 36 nm, which is in agreement with the crystallite size obtained from XRD after corrections, is much smaller than those reported for the powders prepared through the other synthesis methods. The corresponding selected area electron diffraction pattern of the same sample (i.e. $SrBi_2Nb_2O_9$) showed distinct rings, characteristic of an assembly of nano-crystallites as in Fig. 6(b).

4.5. Microstructure

Fig. 7 shows typical SEM micrographs of the polished surfaces of SBN ferroelectrics. All samples have a relatively dense structure, although small voids or pores were found in all samples. The SEM images indicate that the SBN samples have an average grain size of ∼0.67 μm. The grain sizes were calculated using "UTHSCA" image tool software (version 3 @copy right 1995–2002, The University of Texas Health Science Center, San Antonia, USA).

4.6. Dielectric property

Temperature dependency of the dielectric constant and loss factor were obtained at several frequencies at 1 kHz, 100 kHz and 1 MHz for the SBN sintered samples at 900 °C 5 h. The study revealed that the dielectric constant increased gradually

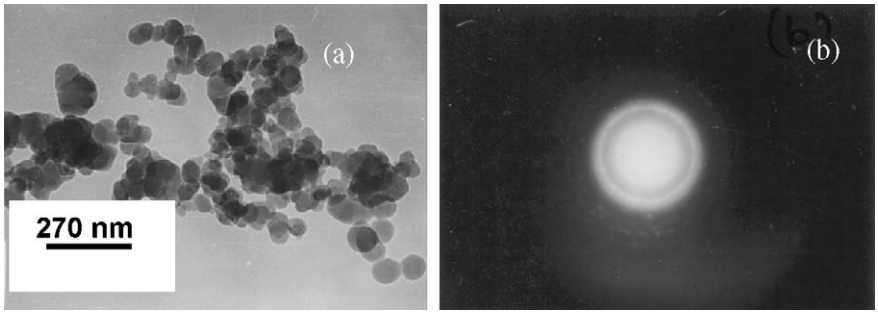

Fig. 6. Bright field TEM of $SrBi_2Nb_2O_9$ calcined at 600 °C and the corresponding SAED pattern.

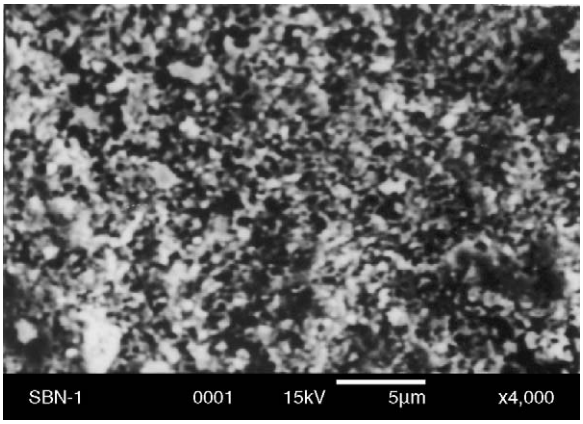

Fig. 7. SEM micrographs of the polished surfaces of $SrBi_2Nb_2O_9$ ferroelectrics sintered at 900 °C for 5 h.

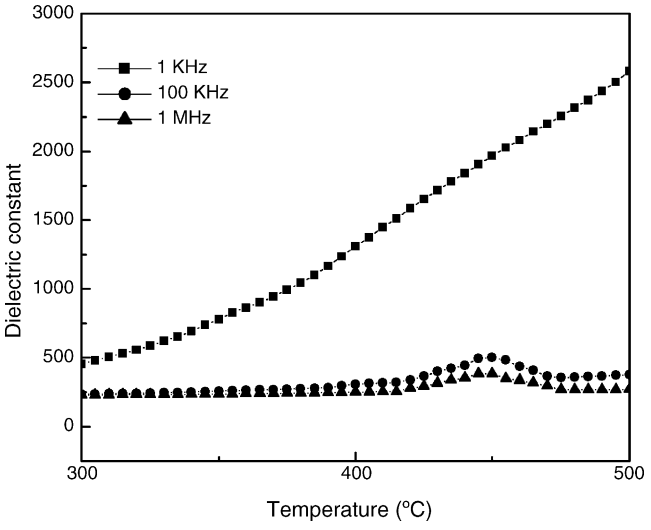

Fig. 8. Dielectric constant as a function of temperature for $SrBi_2Nb_2O_9$ at frequencies 1 kHz, 100 kHz, and 1 MHz.

with temperature and reached a maximum (ε_{max}) at the Curie temperature (T_c) 450 °C (Fig. 8.) which is in agreement with the reported one.[22] ε_{max} value, measured at 100 kHz and 1 MHz were found to be 500 and 384, respectively, but the dielectric constant sharply increased with temperature when measured at frequency 1 kHz; at 450 °C the ε was found to be 1970.

The tangent losses as a function of temperature at 1 kHz, 100 kHz and 1 MHz for SBN were shown in Fig. 9. Tangent losses increased with increasing temperature particularly at temperature higher than ~400 °C. This could be caused by higher concentration of charge carriers (positive and negative vacancies) at higher temperatures. It was noticed that the tangent losses were increased rapidly with temperature at the frequency 100 kHz as shown in Fig. 9.

5. Discussion

Lowering the synthesis temperature of the pure perovskites SBN down to 700 °C has been reported in alkoxide-based

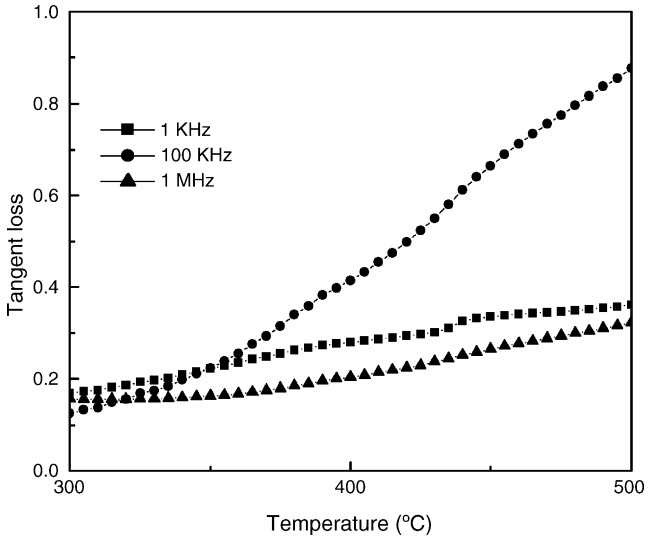

Fig. 9. Tangent loss as a function of temperature for $SrBi_2Nb_2O_9$ at frequencies 1 kHz, 100 kHz and 1 MHz.

sol–gel studies.[9,14] However, the expense and extremely large sensitivity to moisture of Nb- and Bi-alkoxides limit their practical applicability. We therefore emphasize that the important practical and environmentally beneficial aspect of our aqueous solution technique is linked with the economical and safe use of water as a process solvent for the synthesis of SBN. In the case where solution systems involve Bi and Nb, precautions should be taken against formation of precipitates at any stage of the processing, which deteriorates the homogeneity of the system. Our aqueous solution technique is characterized by several aspects, which include: (i) the use of water-resistant Bi-EDTA and Nb-tartarate; (ii) the use of excess TEA relative to metal ions; and (iii) the use of non-toxic water as a process solvent. These allow us to construct a novel aqueous solution system involving Bi and Nb which is usually stable against hydrolysis, thus forming a compositionally homogeneous gelatinous viscous matter rather than precipitation during evaporation of water.

6. Conclusions

The nano-sized layered ferroelectric ceramic-layered $SrBiNb_2O_9$ have been synthesized through the pyrolysis of coordination compounds of metal ions. The powder has good sinter-active properties. The use of Sr-EDTA, Bi-EDTA and Nb-tartarate has been proved very effective for affording a means towards an environmentally friendly aqueous synthesis of the ferroelectric perovskites $SrBi_2Nb_2O_9$ at reduced temperatures (600 °C). Besides that the dielectric properties obtained by this synthetic procedure is significantly high.

Acknowledgement

Authors thank Council of Scientific and Industrial Research, India, for financial support.

References

1. Watanabe, H. and Mihara, T., Preparation of ferroelectric thin films of bismuth layer structured compounds. *Jpn. J. Appl. Phys., Part 1*, 1995, **34**(9B), 5240–5244.
2. de Araujo, C. A. P., Mc Millan, L. D., Cuchiaro, J. D., Scott, M. C. and Scott, J. F., Fatigue-free ferroelectric capacitors with platinum electrodes. *Nature (London)*, 1995, **374**(6523), 627–629.
3. Scott, J. F. and de Araujo, C. A. P., Ferroelectric memories. *Science*, 1989, **246**(4936), 1400–1405.
4. Aurivillius, B., Structures of Bi_2NbO_5F and isomorphous compounds. *Ark. Kemi.*, 1952, **5**, 39–47.
5. Subbarao, E. C., Ferroelectricity in $Bi_4Ti_3O_{12}$ and its solid solutions. *Phys. Rev.*, 1961, **122**(3), 804–807.
6. Xu, Y. H., *Ferroelectric materials and their applications*. Elsevier Science, Amsterdam, 1991.
7. Scott, J. F., High dielectric constant thin films for dynamic random access memories (DRAM). *Annu. Rev. Mater. Sci.*, 1998, **28**, 79–100.
8. Mihara, T., Yoshimori, H., Watanabe, H. and de Araujo, C. A. P., Characteristics of bismuth layered $SrBi_2Ta_2O_9$ thin-film capacitors and comparison with $Pb(Zr, Ti)O_3$. *Jpn. J. Appl. Phys., Part 1*, 1995, **34**(9), 5233–5239.
9. Kato, K., Zheng, C., Finder, J. M. and Dey, S. K., Sol–gel route to ferroelectric layer-structured perovskite SrBi/sub 2/Ta/sub 2/O/sub 9/and SrBi/sub 2/Nb/sub 2/O/sub 9/thin films. *J. Am. Ceram. Soc.*, 1998, **81**(7), 1869–1875.
10. Kakihana, M., Sol–gel preparation of high temperature superconducting oxides. *J. Sol–Gel Sci. Technol.*, 1996, **6**, 7–55.
11. Boyle, T. J., Buchheit, C. D., Rodriguez, M. A., Al-Shareef, H. N., Hernandez, B. A., Scott, B. and Ziller, J. W., Formation of $SrBi_2Ta_2O_9$. Part I. Synthesis and characterization of a novel "sol–gel" solution for production of ferroelectric $SrBi_2Ta_2O_9$ thin films. *J. Mater. Res.*, 1996, **11**(9), 2274–2281.
12. Sakamoto, W., Yogo, T., Kikuta, K., Ogiso, K., Kawase, A. and Hirano, S., Synthesis of strontium barium niobate thin films through metal alkoxide. *J. Am. Ceram. Soc.*, 1996, **79**(9), 2283–2288.
13. Ito, Y., Ushikubo, M., Yokoyama, S., Matsunaga, H., Atsuki, T., Yonezawa, T. and Ogi, K., New low-temperature processing of sol–gel $SrBi_2Ta_2O_9$ thin films. *Jpn. J. Appl. Phys., Part 1*, 1996, **35**(9B), 4925–4929 [regular papers, short notes and review papers].
14. Yi, J. H., Thomas, P., Manier, M., Mercurio, J. P., Jauberteau, I. and Guinebretiere, R., $SrBi_2Nb_2O_9$ ferroelectric powders and thin films prepared by sol–gel. *J. Sol–Gel Sci. Technol.*, 1998, **13**(1/2/3), 885–888.
15. Zanetti, S. M., Araujo, E. B., Leite, E. R., Longo, E. and Varela, J. A., Structural and electrical properties of $SrBi_2Nb_2O_9$ thin films prepared by chemical aqueous solution at low temperature. *Mater. Lett.*, 1999, **40**(1), 33–38.
16. Zhou, Q. F., Chan, H. L. W. and Choy, C. L., Synthesis and properties of ferroelectric $SrBi_2Ta_2O_9$ powder and films prepared by a sol–gel process. *J. Non-Cryst. Solids*, 1999, **254**(1–3), 106–111.
17. Pathak, A., Mohapatra, S., Mohapatra, S., Biswas, S. K., Dhak, D., Pramanik, N. K., Tarafdar, A. and Pramanik, P., Preparation of nanosized mixed-oxide powders. *Am. Ceram. Soc. Bull.*, 2004, **83**(8), 9301–9306.
18. Dhak, D. and Pramanik, P., Particle size comparison of soft-chemically prepared transition metal (Co, Ni, Cu, Zn) aluminate spinels. *J. Am. Ceram. Soc.*, 2005, in press.
19. Rodriguez, M. A., Boyle, T. I., Buchheit, C. D., Tissot, R. G., Drewien, C. A., Hernandez, B. A., *et al.*, Phase formation and characterization of the $SrBi_2Ta_2O_9$ layered-perovskite ferroelectric. In *Eighth International Symposium on Integrated Ferroelectrics* (Pt. 1), 1996. *Integrated Ferroelectrics* 1997, **14**(1–4), 201–210.
20. Rodriguez, M. A., Boyle, T. J., Hernandez, B. A., Buchheit, C. D. and Eatough, M. O., Formation of $SrBi_2Ta_2O_9$. Part II. Evidence of a bismuth-deficient pyrochlore phase. *J. Mater. Res.*, 1996, **11**(9), 2282–2287.
21. Warren, B. E., *X-ray diffraction*. Addison–Wesley, Reading, MA, 1969, pp. 253, 258;
    Warren, B. E., *Amorphous materials*. Wiley, New York, 1973, pp. 687, 635;
    Scherrer, P., *GÖttinger Nachichent 2*, 1918, **98**.
22. Harihara Venkataraman, B. and Varma, K. B. R., Frequency-dependent dielectric characterise of ferroelectric $SrBi_2Nb_2O_9$ ceramics. *Solid State Ion.*, 2004, **167**, 197–202.